AIP | Applied Physics Letters

Long wavelength emission of InGaAsN/GaAsSb type II "W" quantum wells

J.-Y. Yeh, L. J. Mawst, A. A. Khandekar, T. F. Kuech, I. Vurgaftman et al.

Citation: Appl. Phys. Lett. **88**, 051115 (2006); doi: 10.1063/1.2171486
View online: http://dx.doi.org/10.1063/1.2171486
View Table of Contents: http://apl.aip.org/resource/1/APPLAB/v88/i5
Published by the American Institute of Physics.

Long wavelength emission of InGaAsN/GaAsSb type II "W" quantum wells

J.-Y. Yeh[a] and L. J. Mawst
University of Wisconsin-Madison, Department of Electrical and Computer Engineering, 1415 Engineering Drive, Madison, Wisconsin 53706

A. A. Khandekar and T. F. Kuech
University of Wisconsin-Madison, Department of Chemical and Biological Engineering, 1415 Engineering Drive, Madison, Wisconsin 53706

I. Vurgaftman and J. R. Meyer
Code 5613, Naval Research Laboratory, Washington, DC 20375

N. Tansu
Center for Optical Technologies, Department of Electrical and Computer Engineering, Lehigh University, Bethlehem, Pennsylvania 18015

(Received 1 August 2005; accepted 13 December 2005; published online 2 February 2006)

Low temperature (30 K) long wavelength photoluminescence emission ($\lambda = 1400-1600$ nm) from metalorganic chemical vapor deposition grown InGaAsN–GaAsSb type II "W" quantum wells (QWs), on GaAs substrates has been demonstrated. Thin layers (2–3 nm) and high antimony-content (30%) GaAsSb were utilized in this study for realizing satisfactory wave function overlap and long wavelength emission. Tensile strained GaAsP barriers effectively improve the material structural and luminescence properties of the compressive strained active region. Room temperature photoluminescence data show that the type-II QW design is a promising candidate for realizing long wavelength GaAs-based diode lasers beyond 1500 nm. © *2006 American Institute of Physics*. [DOI: 10.1063/1.2171486]

For superior optical communication system performance and reduced cost, long wavelength (~1300–1550 nm) GaAs-based diode lasers have drawn much attention over the years. The quaternary dilute nitride material InGaAsN represents one of the strongest candidates for 1300 nm emitting diode lasers.[1,2] However, extending the wavelength beyond 1300 nm leads to serious device performance degradation as more nitrogen is introduced into the InGaAsN active region.[3–5] Recently, we proposed a novel approach with an InGaAsN–GaAsSb type II quantum well (QW) active region for realizing GaAs-based diode lasers with emission wavelengths beyond $\lambda = 1500$ nm.[6] This novel approach utilizes the type II band alignment between InGaAsN and GaAsSb. Previous InGaAs–GaAsSb type II QW lasers and photoluminescence studies have been reported. The emission wavelengths were generally limited to 1200–1400 nm, however, mainly due to the maximum lattice strain that the structures can accommodate and the large energy band gap of InGaAs.[7–9] In this study, we utilize the radiative recombination processes between electrons in the InGaAsN conduction band and holes in the GaAsSb valence band. The spatially indirect type II transitions yield longer-wavelength emission than any type I transition from the individual layers. Accordingly, optimizing the electron and hole wave function overlap is essential, as it significantly impacts the radiative efficiency and differential gain of the structure. With the InGaAsN–GaAsSb type II QW design, emission wavelength can be engineered over a wide range, and reasonable wave function overlap can be obtained with a thin QW. The deep potential wells also provide good carrier confinement, which is expected to result in favorable temperature performance of the device characteristics. In addition, by utilizing InGaAsN with high indium content, instead of GaAsN, the required nitrogen content can be greatly reduced, which is beneficial to the material quality and laser properties.

In this study, we investigated a type II QW structure, consisting of a GaAsSb hole QW sandwiched by two InGaAsN electron QWs to form the "W" configuration.[6] Previously, type II "W" active regions grown on GaSb substrates have also been employed for achieving some of the leading III-V interband lasers for the mid-IR regime ($\lambda = 3-5$ μm).[10] Figure 1 shows the schematic band diagram of the "W" shape InGaAsN–GaAsSb active region. The "W" structure design preserves a superior wave function overlap, two-dimensional density of states[10] and a possible mechanism for Auger recombination suppression.[10,11] Design studies on the "W" structure have indicated that the electron and hole wave function overlap is about 50%, and that emission

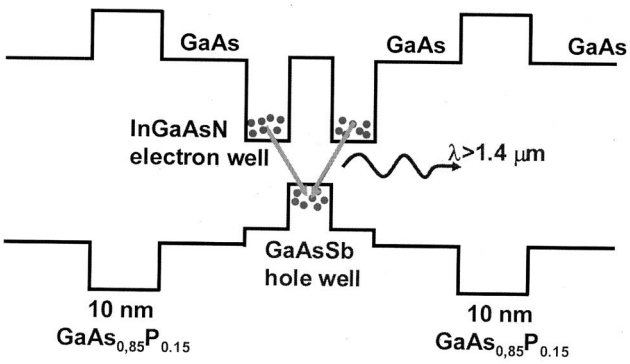

FIG. 1. Schematic band diagram of the InGaAsN–GaAsSb type II "W" QW structure. GaAsP layers are employed for strain compensation purposes. The InGaAsN and GaAsSb thicknesses are 2.5 and 2 nm, respectively.

[a]Author to whom correspondence should be addressed; electronic mail: mawst@engr.wisc.edu

wavelengths as long as 2 μm should be achievable. Ideally, the GaAsSb and InGaAsN layers should be thin to maximize the wave function overlap. On the other hand, the current material epitaxy technology limits the minimum achievable layer thickness. In this work, the InGaAsN and GaAsSb thicknesses are kept at 2–3 nm, the practical range proposed by the theoretical study.[6] Tensile-strained barriers of $GaAs_{0.85}P_{0.15}$ have been employed to compensate the compressively strained "W" active region. This strain compensation design is especially desirable in multiple-stage structures for maximizing the laser modal gain. Optimization of the layer thickness and tensile strain of the GaAsP barriers leads to significant improvements in both the photoluminescence (PL) intensity and the full width half maximum (FWHM). The samples grown for this study contain a single "W" active region located at the center of a 300-nm-wide GaAs separate confinement heterostructure region. Thin $Al_{0.65}Ga_{0.35}As$ top- and bottom-cladding layers (150 nm) are included for better carrier and optical confinement.

The structures were grown by metalorganic chemical vapor deposition (MOCVD) at an active region growth temperature of 530 °C and reactor pressure of 100 mbar. Trimethylgallium, trimethylaluminum and trimethylindium were the group III precursors materials, and AsH_3, PH_3, trimethylantimony, and U-dimethylhydrazine (U-DMHy) were the group V precursors. The solid phase material compositions of InGaAsN and GaAsSb were determined by high-resolution x-ray diffraction (HRXRD) experiments with the layer thickness information obtained from transmission electron microscope images. For GaAsSb, a low V/III ratio of 1.34 (gas phase Sb/V=85%) was utilized, leading to the high antimony solid content of 30% that is essential for achieving long wavelength emission. The growth rate under this condition was calibrated to be 90 Å/min. The gas-switching scheme was studied previously and utilized here for achieving good GaAsSb interfaces.[12] Rough and graded interfaces can greatly deteriorate the luminescence intensity from the type II QW structure, due to the nature of the spatially indirect transition. For InGaAsN, the indium content was 37% and the N/V ratio (mole flow ratio of DMHy and total group V in gas phase) was in the 0.994–0.996 range, corresponding to a solid-phase nitrogen content of approximately 2%. In general, we utilized a very small $[AsH_3]$/III ratio (<10) for growing InGaAsN to allow for sufficient nitrogen incorporation. To characterize the grown QW optical quality, room temperature and low temperature PL measurements (30 K) were conducted with an argon-ion laser ($\lambda \sim 514.5$ nm) as the excitation source. Figure 2 shows the (0 0 4) *x*-ray ω-2θ diffraction pattern of a three-stage InGaAsN–GaAsSb "W" structure. Between each stage, GaAs and tensile strained GaAsP were employed as barriers to separate the highly strained active regions. The two broad envelope modulations represent the diffraction peaks from the individual InGaAsN and GaAsSb layers, as pointed out in the figure. They overlap with the Pendellösung fringes, which result from the diffraction of the periodic layer structure, forming the x-ray diffraction pattern shown in Fig. 2. The distinct fringe pattern indicates good crystal and interface quality of the highly strained materials.

Figure 3(a) shows the 30 K PL spectrum of three as-grown InGaAsN–GaAsSb type II "W" QW structures with various nitrogen contents in the InGaAsN. The InGaAsN thickness is fixed at 2.5 nm, and the thickness of the

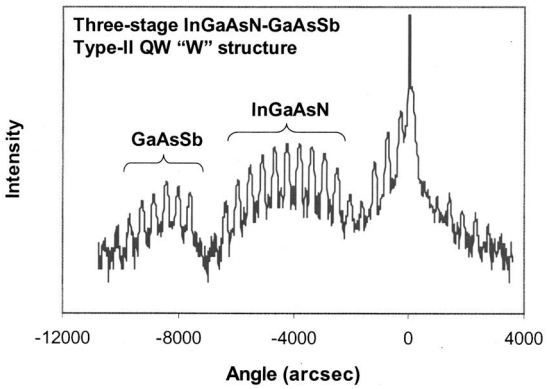

FIG. 2. The high-resolution x-ray ω-2θ diffraction pattern, along the (0 0 4) direction, for a three-stage InGaAsN–GaAsSb "W" structure. The two envelopes are induced by the GaAsSb and InGaAsN layers. The distinct fringe pattern confirms the high quality of the grown materials and interfaces, in spite of the large lattice mismatch ($\sim 2\%$).

$GaAs_{0.7}Sb_{0.3}$ layers is 2 nm. The N/V ratios for these three samples are 0.994, 0.995 and 0.996, and the corresponding emission wavelengths are 1425, 1480 and 1620 nm, respectively. Without nitrogen, the peak emission wavelength for the InGaAs–GaAsSb type II QW at 30 K is 1260 nm. With more than 2.2% nitrogen (N/V=0.996), the longest emission wavelength is extended to 1620 nm, indicating a significant redshift of 220 meV due to the nitrogen-induced band gap bowing. The PL spectral FWHM is increased from 30 meV for the nitrogen-free sample to 78–88 meV for the samples with high nitrogen content. The significant degradation of the

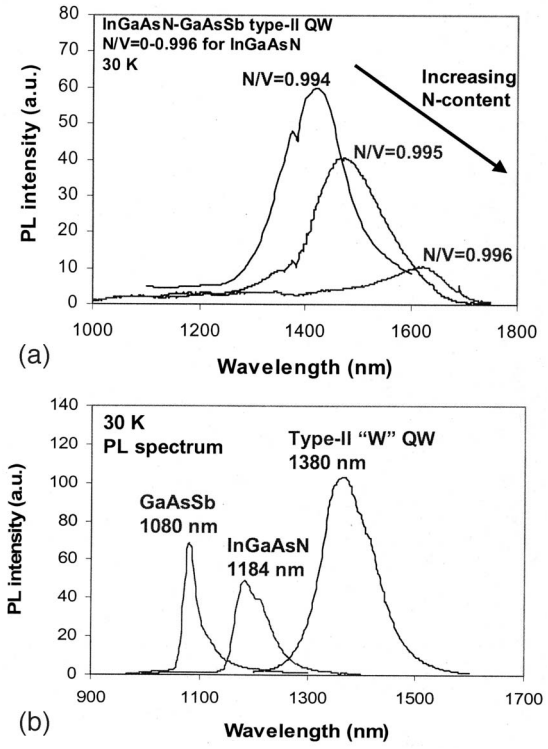

FIG. 3. (a) A 30 K PL spectrum of the InGaAsN–GaAsSb type II QW "W" structures grown with various gas phase N/V ratios ranging from 0.994 to 0.996. A substantial wavelength redshift was observed with increasing nitrogen content in the InGaAsN QW. (b) PL comparison between the type II structure and InGaAsN and GaAsSb type I QWs, showing clear evidence for longer-wavelength emission when the type II band alignment is employed.

PL intensity and FWHM for the 1620 nm sample is presumably due to onset of the three-dimensional growth mode under such an extremely high N/V ratio, which is further verified by the HRXRD experiments.

To confirm that the light emission is a result of electron-hole radiative recombination via the type II transition, InGaAsN–GaAs single QW and GaAsSb–GaAs single QW structures (keeping the same material compositions and QW thickness as the layers in the "W" structure) were grown with the N/V ratio equal to 0.995. Those two QW structures and the type II QW were *in situ* annealed at 640 °C for 25 min. The 30 K PL emission wavelengths for all three are shown in Fig. 3(b). The peak wavelengths for the InGaAsN and GaAsSb QWs are 1184 and 1080 nm, respectively, while the peak for the type II "W" QW occurs near 1380 nm. The significant wavelength extension obtained for the InGaAsN–GaAsSb "W" structure confirms that the transition in this active region is type II. The emission wavelength of 1380 nm for the annealed sample is shorter than that measured for the as-grown sample (1480 nm), shown in Fig. 3(a), due to the well-known blueshift effect that occurs when InGaAsN is thermally annealed. In addition to the wavelength blueshift, the PL intensity of the annealed sample is six times higher than that of the as-grown sample. According to our energy band structure simulation by the ten band $k \cdot p$ formalism,[7] the calculated 30 K emission wavelengths of the InGaAsN–GaAs QW, GaAsSb–GaAs QW, and type II "W" structure are 1054, 1081, and 1345 nm, respectively. That the predicted emission wavelengths for the samples containing InGaAsN layers are shorter than the experimental results may be due to atomic ordering in the InGaAsN, which is not accounted for in the simulation. Since the thermal annealing condition utilized here does not saturate the blueshift, a higher-temperature anneal may induce further blueshift and hence closer agreement with modeling. In addition, graded InGaAsN–GaAsSb interfaces may also contribute to the deviation between theory and experiment.

This type II QW structure also displayed long wavelength emission at room temperature. Figure 4 shows the room temperature PL spectrum of the InGaAsN–GaAsSb "W" structure with N/V of 0.996 and annealed at 720 °C. Under high excitation power density (100 W/cm^2), the emission wavelength is near 1600 nm. The wavelength shift from 1580 nm at 30 K to 1600 nm at room temperature results from the combination of a redshift with increasing temperature and a blueshift at higher excitation power density (and higher carrier density in the QW).[13] This room temperature PL result indicates that the type II QW design is a promising candidate for realizing long wavelength GaAs-based diode lasers that emit beyond 1500 nm.

In summary, long wavelength emission ($\lambda \sim 1400-1600$ nm) has been observed from InGaAsN–GaAsSb type II "W" QW structures grown by metalorganic chemical vapor deposition. With optimized growth conditions, high antimony content GaAsSb was achieved for extension of the wavelength. The "W" structure's layer thickness of 2–3 nm is in the desired range, according to theoretical simulations. The x-ray and PL studies show good crystalline and optical luminescence properties of the grown structures. Successful demonstration of room temperature luminescence at 1600 nm from the type II QW identifies its potential for realizing GaAs-based diode lasers emitting beyond 1400 nm.

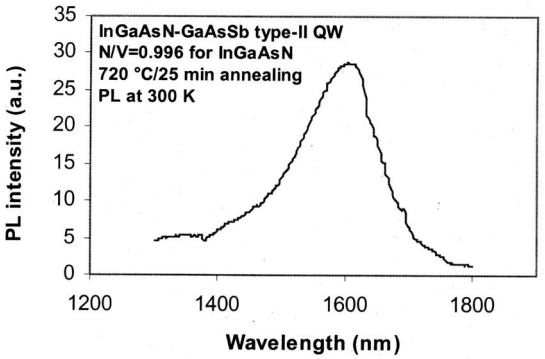

FIG. 4. Room temperature (300 K) PL spectrum of the InGaAsN–GaAsSb type II "W" structure.

The work at University of Wisconsin-Madison was supported by the Army Research Office.

[1] N. Tansu, N. J. Kirsch, and L. J. Mawst, Appl. Phys. Lett. **81**, 2523 (2002).
[2] A. Y. Egorov, D. Bernklau, D. Livshits, V. Ustinov, Z. I. Alferov, and H. Riechert, Electron. Lett. **35**, 1643 (1999).
[3] J.-Y. Yeh, L. J. Mawst, and N. Tansu, J. Cryst. Growth **272**, 719 (2004).
[4] M. Yokozeki, J. Mitomo, Y. Sato, T. Hino, and H. Narui, Electron. Lett. **40**, 1060 (2004).
[5] F. Hohnsdorf, J. Koch, S. Leu, W. Stolz, B. Borchert, and M. Druminski, Electron. Lett. **35**, 571 (1999).
[6] I. Vurgaftman, J. R. Meyer, N. Tansu, and L. J. Mawst, Appl. Phys. Lett. **83**, 2742 (2003).
[7] S. W. Ryu and P. D. Dapkus, Electron. Lett. **38**, 564 (2002).
[8] M. Kudo, K. Ouchi, J. Kasai, and T. Mishima, Jpn. J. Appl. Phys., Part 2 **41**, 1040 (2002).
[9] J. F. Klem, O. Blum, S. R. Kurtz, J. Fritz, and K. D. Choquette, J. Vac. Sci. Technol. B **18**, 1605 (2000).
[10] J. R. Meyer, C. A. Hoffman, F. J. Bartoli, and L. R. RamMohan, Appl. Phys. Lett. **67**, 757 (1995).
[11] M. E. Flatte, J. T. Olesberg, S. A. Anson, T. F. Boggess, T. C. Hasenberg, T. H. Miles, and C. H. Grein, Appl. Phys. Lett. **70**, 3212 (1997).
[12] B. E. Hawkins, A. A. Khandekar, J.-Y. Yeh, L. J. Mawst, and T. F. Kuech, J. Cryst. Growth **272**, 686 (2004).
[13] W. W. Chow, O. B. Spahn, H. C. Schneider, and J. F. Klem, IEEE J. Quantum Electron. **37**, 1178 (2001).